



HAL
open science

Impact of DM misregistration for NCPA compensation in HARMONI's SCAO system

Douglas Harvey, Noah Schwartz, Charlotte Bond, Jean-François Sauvage

► **To cite this version:**

Douglas Harvey, Noah Schwartz, Charlotte Bond, Jean-François Sauvage. Impact of DM misregistration for NCPA compensation in HARMONI's SCAO system. Adaptive Optics for Extremely Large Telescopes 7th Edition, ONERA, Jun 2023, Avignon, France. <10.13009/AO4ELT7-2023-064>. <hal-04402856>

HAL Id: hal-04402856

<https://hal.science/hal-04402856v1>

Submitted on 18 Jan 2024

HAL is a multi-disciplinary open access archive for the deposit and dissemination of scientific research documents, whether they are published or not. The documents may come from teaching and research institutions in France or abroad, or from public or private research centers.

L'archive ouverte pluridisciplinaire HAL, est destinée au dépôt et à la diffusion de documents scientifiques de niveau recherche, publiés ou non, émanant des établissements d'enseignement et de recherche français ou étrangers, des laboratoires publics ou privés.



HAL Authorization



Impact of DM misregistration for NCPA compensation in HARMONI's SCAO system

Douglas Harvey^{a,*}, Noah Schwartz^a, Charlotte Bond^a, Jean-François Sauvage^{b,c}

^aUK Astronomy Technology Centre, Blackford Hill, Edinburgh EH9 3HJ, United Kingdom;

^bDOTA, ONERA, F-13661 Salon cedex Air - France; ^cMarseille Univ, CNRS, LAM, Laboratoire d'Astrophysique de Marseille, Marseille, France

ABSTRACT

Non-Common Path Aberration (NCPA) compensation is crucial for good image quality, especially for high contrast operations. In SCAO mode HARMONI will use a calibration deformable mirror (DM) in conjunction with of low-order DM to calibrate and correct the NCPAs between the wavefront sensor path and the science detectors. However, constraints in the optical design requires the low-order DM to be rotated with respect to the calibration DM, and places them several metres apart, leading to misregistrations between the two DMs. In this paper, we present the results of Monte Carlo simulations to determine how residual WaveFront Errors (WFEs) between the DMs vary with these misregistrations. When controlling the first 50 Zernike modes we find residual WFEs to be $\leq 3\%$ for all rotation angles and pupil shifts ≤ 0.5 of a DM pitch (5% of the pupil). Small magnification errors contribute little to the overall error. This result confirms the Low-Order DM can compensate for NCPAs and deliver a flat wavefront to the Pyramid wavefront sensor (PyWFS) even with relatively large misregistrations.

Keywords: Extremely Large Telescope, Adaptive Optics, Deformable Mirror, HARMONI, Registration

1. INTRODUCTION

HARMONI¹ is the first light visible and near-IR integral field spectrograph for the Extremely Large Telescope (ELT). It covers a large spectral range from 450 nm to 2450 nm with resolving powers from 3500 to 18000 and spatial sampling from 60 mas to 4 mas. It can operate in two Adaptive Optics modes – SCAO (including a High Contrast capability) and LTAO – or with NAO. The project is preparing for Final Design Reviews.

HARMONI will use image slicers to provide spectra over a single contiguous field measuring 204x152 spaxels in size. Calibration light can be fed into the instrument via a deployable calibration system upstream of the Focal Plane Relay System (FPRS). Figure 1 shows a schematic of the HARMONI instrument with the different modules labelled.

Wavefront sensing for the SCAO mode is mainly provided by a Pyramid WaveFront Sensor (PyWFS). The high sensitivity of the PyWFS comes at the expense of a small dynamic range, limiting its ability to compensate for Non-Common Path Aberrations (NCPAs) through offsets of the operating point (i.e., using reference slopes). As NCPA compensation is crucial for good image quality, especially for high contrast operations, a low-order loop upstream of the PyWFS will be implemented to correct for NCPAs. This loop consists of a Shack-Hartman WFS (SH-WFS) controlling a Low-Order DM (LODM). The reference slopes of the SH-WFS will be modified so that the LODM absorbs large low-order NCPAs and delivers a flat wavefront to the PyWFS.

*douglas.harvey@stfc.ac.uk

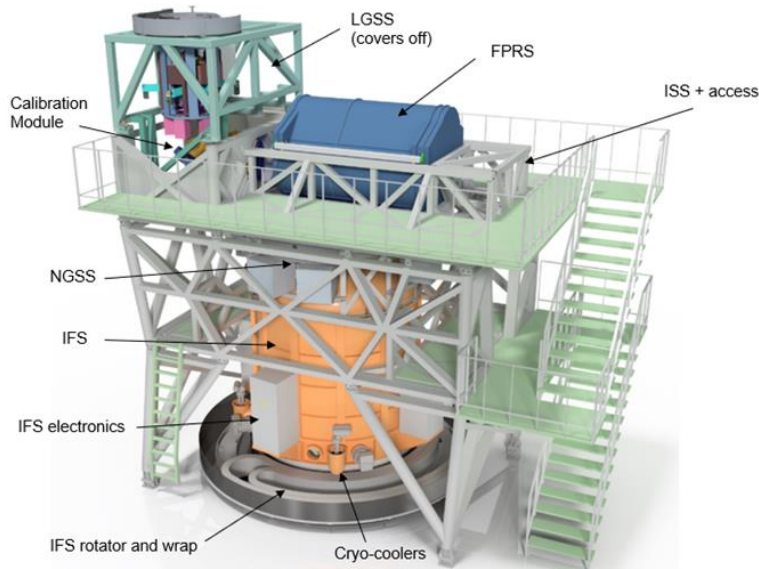


Figure 1-1: Rendering of the HARMONI structure highlighting some key elements and modules. The Calibration Module can be deployed into the instrument focal plane to inject calibration light into the rest of the system.

A Calibration DM (CalDM) will be used to calibrate NCPAs and determine the SH-WFS's reference slopes. However, The LODM is in the NGS system (see Figure 1-1) and rotates with the IFS, while the CalDM is located in the Calibration Module (several metres from the NGS system) and does not rotate. The distance between the LODM and the CalDM and the rotation of the IFS leads to misregistration between the two DMs.

1.1 Calibration module

Figure 1-2 presents the Calibration Module (CM) main structures and components. The CM sits just in front of the telescope focal plane and injects calibration light into the system. It can be completely withdrawn to allow normal observations. The calibration module is comprised of three separate units: the IFS calibration unit, the Geometric calibration unit (GCU), and the AO calibration unit² (AOCU). The AO fold mirror (AOFM) directs the AOCU light into the instrument. Two focus stages enable the AOCU to be moved into position to inject light into the system (moving AOCU and AOFM at the same time) and to move the AOCU linearly in the field (moving the AOCU stage while keeping the AOFM in place).

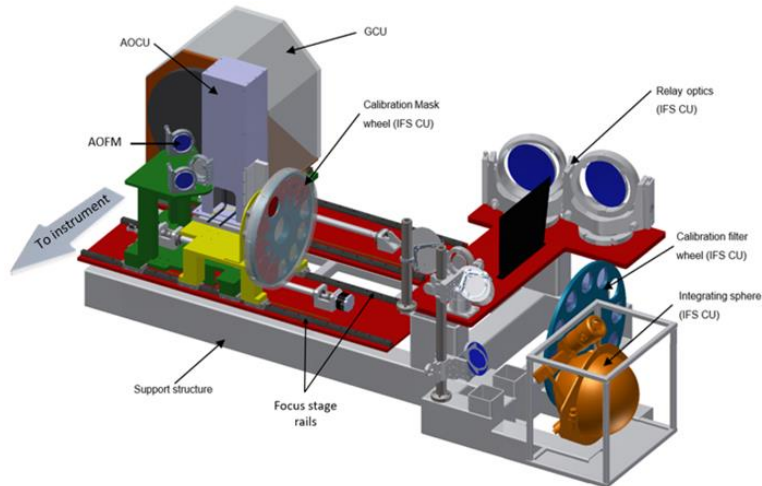


Figure 1-2: Overall view of the Calibration Module, showing the AOCU, AO fold mirror (AOFM), and the 2 focus stages (the positioning stage in green, and the focus stage in yellow).

The AOCU contains a Calibration DM (CalDM) which is used to introduce aberrations into the light path to probe the whole field of view (FoV) for NCPAs. To accurately calibrate the system, CalDM must be able to patrol the entire science FoV. However, even combining CalDM's tip-tilt capability with linear movements of the AOCU, parts of the field would not be covered. To allow the whole field to be covered, linear movement of the AOCU (using the focus stages, see Figure 1-2) is combined with rotation of the IFS.

1.2 The SCAO system

Figure 1-3 illustrates the HARMONI SCAO system both in regular operation and in calibration mode. In operation, light is provided by a guide star, with M4 (the ELT's deformable mirror and M5 (the ELT's tip-tilt mirror) providing correction for atmospheric turbulence. In calibration mode, light is provided by the calibration unit.

NCPAs are aberrations originating from within the instrument. The aberrations must be measured and compensated for in order to reduce WFE to the level required for scientific observations. For HARMONI's SCAO system to provide AO correction for the science instrument, NCPAs must be compensated. However, the low dynamic range of the PyWFS makes it difficult to compensate NCPAs using offsets of its operating point. This limitation is overcome using a low-order loop which consists of a Shack-Hartmann WFS (SH-WFS) and LODM. Low-order NCPAs (up to 50 Zernike modes) are absorbed by setting the reference slopes of the SH-WFS, providing a flat wavefront to the PyWFS.

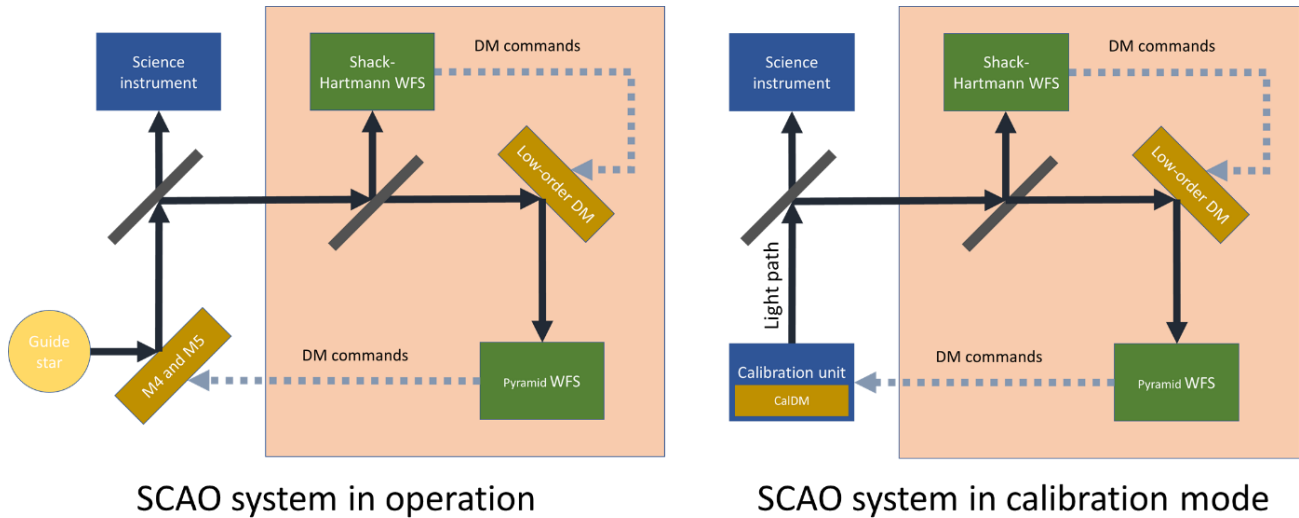


Figure 1-3: Illustration of the HARMONI SCAO system in operation and in calibration mode.

During calibrations, the CalDM is used to probe NCPAs and the respective SH-WFS reference slopes will be recorded for NCPA compensation. Ideally, the LODM would perfectly correct aberrations introduced by the CalDM, leaving a flat wavefront. However, in operation the Natural Guide Star System (NGSS) rotates relative to the science instrument and the design places the DMs far apart, with the potential to introduce a misregistrations between the two DMs. The actual pupil size on the DM (20 mm) is slightly smaller than the DM aperture itself (22.5 mm) providing some margin for misalignments. The aim of this research was to simulate the CalDM-LODM system and quantify the errors introduced by misregistration.

2. SIMULATION STRATEGY

2.1 Simulation of the CalDM and LODM

The CalDM and the LODM will be ALPAO 97-25 large stroke DMs. We approximate the measured influence functions by a Gaussian, fitting both their location (through a slight magnification) and inter-actuator coupling. Figure 2-1 compares the resulting WFE after a range of Zernike modes are corrected using the original ALPAO influence functions and the Gaussian influence functions. It confirms a close match in terms of residual WFE for modes 2 to 50. The NCPAs only need to be corrected up to mode 50, so performance for higher-order modes can be ignored.

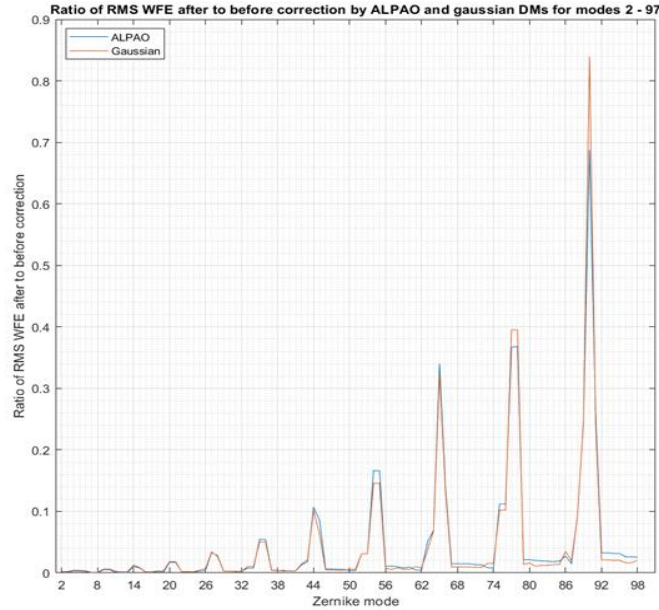


Figure 2-1: Comparison of resulting WFE after Zernike modes 2 to 96 are corrected by the ALPAO (blue) and Gaussian (red) influence function.

As expected, the large fitting errors both for the ALPAO and Gaussian influence functions correspond to Zernike modes with high spatial frequencies around the edge of the aperture (examples for selected modes are shown in Figure 2-2 below).

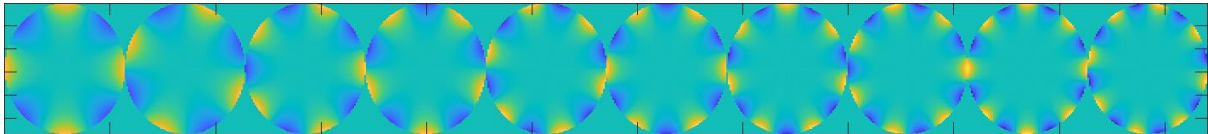


Figure 2-2: Selection of Zernike modes leading to a poor correction by the DM due to the high spatial frequency around the edge: From left to right Zernike mode: 14, 15, 20, 21, 27, 28, 35, 36, 44, and 45.

2.2 General simulation strategy

The simulation consists of 2 main objects: LODM, which can have any combination of linear shift, rotation and magnification applied to it, and CalDM which is fixed. To isolate misregistration errors from fitting errors, we project the Zernike modes onto CalDM and record its actuator coefficients (i.e., dm.coefs, see Figure 2-4), then use these coefficients to define a set of projected modes (“P-Zernike”). These P-Zernike modes were used in all simulations. The shape of LODM is obtained via projection to avoid any additional measurement errors and concentrate only on misregistration errors.

There are 3 different types of aperture (shown in Figure 2-3) imposed by the optical design: a fixed 22.5 mm aperture corresponding to CalDM on which the P-Zernike modes are defined, a 22.5 mm aperture corresponding to LODM which may be shifted with respect to the CalDM aperture, and finally a fixed 20 mm aperture on which performance is measured. This 20 mm aperture corresponds to the pupil as defined by the optical design. Both DMs have a 22.5 mm clear aperture.

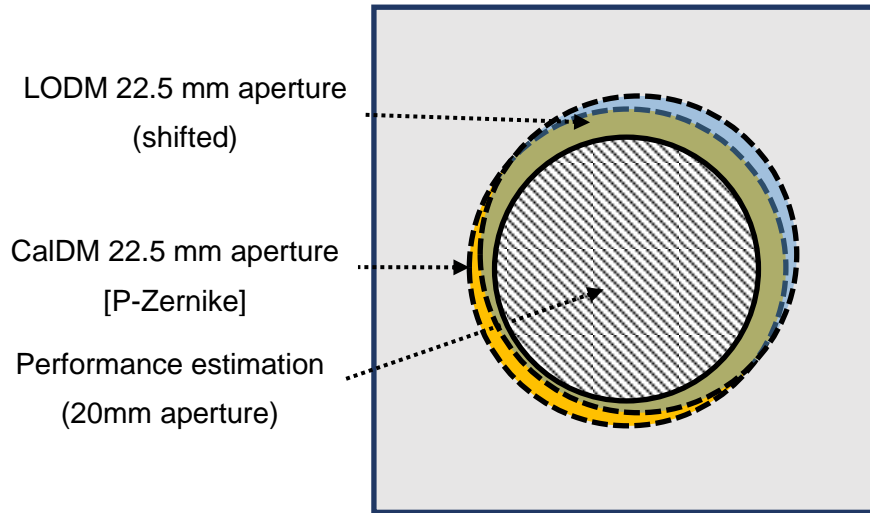


Figure 2-3 Illustration of the 3 apertures as defined by the optical design (CalDM, LODM and a smaller 20 mm aperture used for performance estimation).

In each run of the simulation either a single P-Zernike or combination of multiple P-Zernikes is created on the CalDM and a misregistration is applied to the LODM. Finally, the equivalent shape of the LODM is calculated via projection. As illustrated in Figure 2-4, an initially flat wavefront is propagated from CalDM (giving φ_{NCPA} , the NCPA wavefront) to LODM (giving $\varphi_{Residual}$, the residual wavefront after correction). The RMSE ratio is then calculated over the 20 mm aperture:

$$RMSE_{ratio} = \frac{RMS(\varphi_{Residual})}{RMS(\varphi_{NCPA})} \quad (1)$$

In other words, $RMSE_{ratio} = 0$ when no misregistrations are present i.e., when LODM perfectly corrects the aberrations introduced by CalDM. Equally, $RMSE_{ratio} = 1$ when LODM has not reduced the NCPA WF at all i.e., $\varphi_{NCPA} = \varphi_{Residual}$.

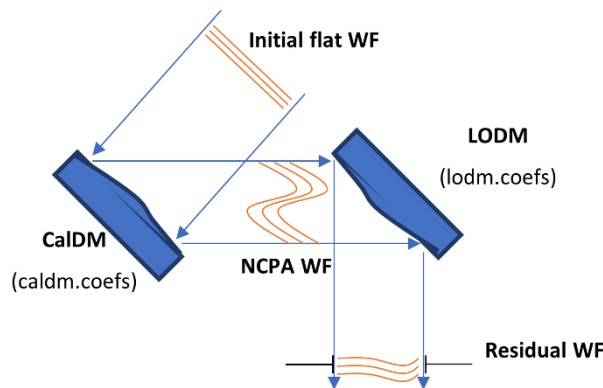


Figure 2-4: Illustration of the simulation method. A P-Zernike mode is created with CalDM, it is then propagated to a misregistered LODM, and performance is estimated on a 20 mm pupil. caldm.coefs are the actuator coefficients of CalDM, lodm.coefs are the actuator coefficients of LODM (calculated via a projection).

3. SIMULATION RESULTS

In this section, we investigate the impact of rotation and linear shift of one DM relative to another. We have found that magnification has little to no impact on performance and has been omitted from this paper. All simulations were performed using the Object-Oriented Matlab Adaptive Optics (OOMAO³) Toolbox.

3.1 Linear misregistrations

To investigate the effects of linear misregistration on individual P-Zernike modes, the LODM was shifted linearly in a series of steps up to 1 actuator pitch (2.52 mm) from its initial position (perfectly registered with the CalDM). Figure 3-1 shows a heatmap of the resulting $RMSE_{ratio}$ for the first 50 P-Zernike modes as a function of linear shift distance. As expected, there are large spikes in the $RMSE_{ratio}$ for modes with high spatial frequencies along the edges of the aperture (see Figure 2-2 for examples). Other modes produce smaller errors, typically <15%.

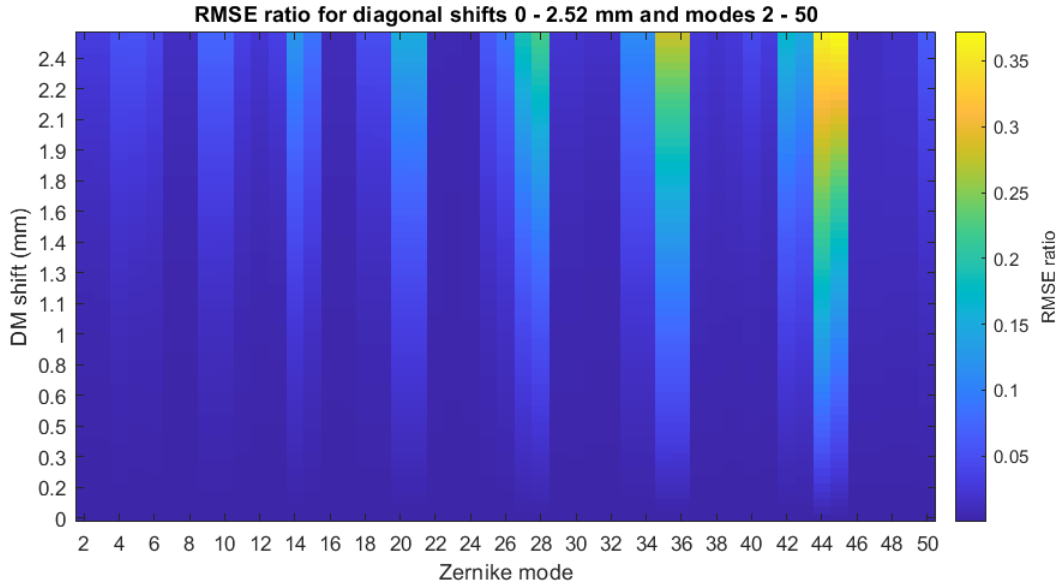


Figure 3-1: Heatmap of $RMSE_{ratio}$ as a function of linear shift distance for P-Zernike modes 2 to 50.

Figure 3-2 shows the residual phase ($\varphi_{Residual}$) after LODM attempts to correct mode 44, with a series of increasingly large linear shifts to the left applied to the LODM. The LODM struggles to fit the shifted high spatial frequencies along the right-hand edge of the aperture, leading to high levels of errors.



Figure 3-2: Phases resulting from increasingly large horizontal shifts of the LODM with P-Zernike mode 44 on the CalDM.

As seen from Figure 3-1, the worst modes (44 and 45) lead to an error >35% for shifts of an actuator pitch. However, real NCPAs are unlikely to exhibit high-order modes with large amplitude. To investigate the effects of linear misregistration for more realistic NCPAs, we use a combination of P-Zernikes following an f^{-2} spectrum and shift LODM randomly in both X and Y up to 1 actuator pitch (2.52 mm). **Error! Reference source not found.** and

Figure 3-4 present the $RMSE_{ratio}$ (see Equation (1)) resulting from these random shifts. We plot this as a function of $RMSE_{quadSum}$ (see Equation (2)), which is the quadratic sum of the $RMSE_{ratio}$ from separately applying X and Y linear misregistrations.

$$RMSE_{quadSum} = \sqrt{RMSE_{ratio_x}^2 + RMSE_{ratio_y}^2} \quad (2)$$

Where $RMSE_{ratio_x}$ and $RMSE_{ratio_y}$ result from calculating the $RMSE_{ratio}$ with only the x or y component of the misregistration applied separately. It was found that, so long as linear shifts are kept small, or approximately below 0.1 to 0.2 pitch, $RMSE_{ratio} \approx RMSE_{quadSum}$. The errors increase more rapidly beyond that. For linear shift of 0.1 pitch, the errors are kept below 0.25%. They increase up to 10% for large shifts of 1 actuator pitch.

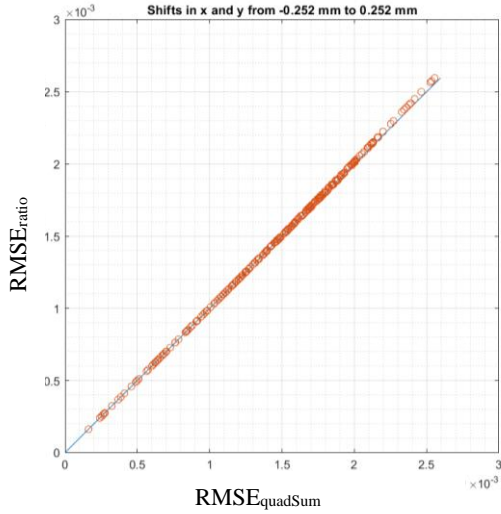


Figure 3-3: $RMSE_{ratio}$ of individual modes added in quadrature against $RMSE_{ratio}$ of combined modes. Random shifts up to 0.1 actuator pitch (0.252 mm). NCPA following f^{-2} spectrum.

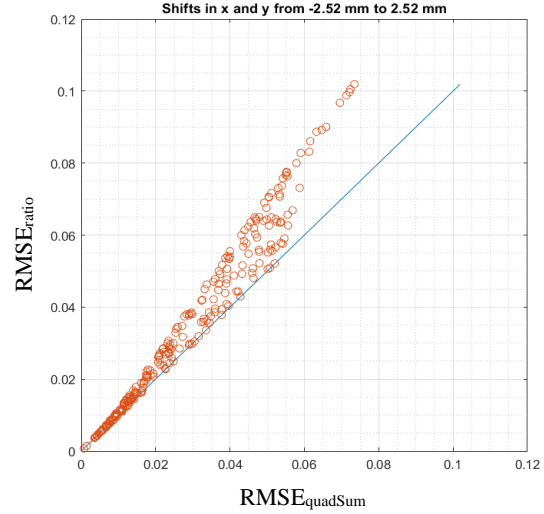


Figure 3-4: $RMSE_{ratio}$ of individual modes added in quadrature against $RMSE_{ratio}$ of combined modes. Random shifts up to 1 actuator pitch (2.52 mm). NCPA following f^{-2} spectrum.

3.2 Rotational misregistrations

Similarly, to the investigation of linear misregistrations described above, rotational misregistration was investigated by rotating LODM with respect to CalDM in steps from 0° to 90° for each P-Zernike mode from 2 to 50. Figure 3-5 **Error! Reference source not found.** shows a similar heatmap to Figure 3-1, but with rotations as opposed to linear shifts. The spikes in $RMSE_{ratio}$ for P-Zernike modes with high spatial frequencies around the edge of the aperture that were present with linear shifts are also present in this case. It can also be seen that, for rotation angles a few degrees from a perfectly registered position, the resulting $RMSE_{ratio}$ is close to 0, while for angles larger than this the $RMSE_{ratio}$ is approximately constant for all modes (except 45 and 46, however these high-order modes are expected to have low amplitude).

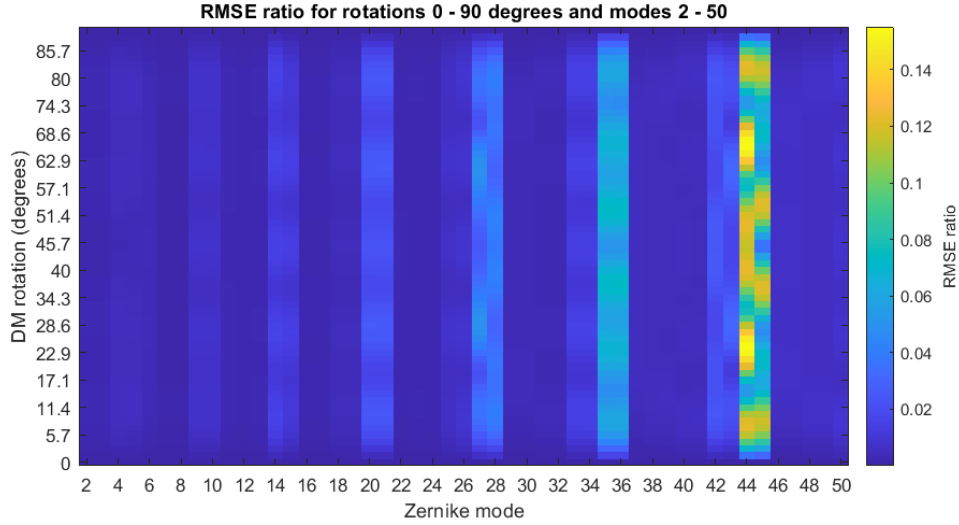


Figure 3-5: Heatmap of RMSEratio as a function of rotation angle for P-Zernike modes 2 to 50.

3.3 Combination of misregistrations

Figure 3-6 shows the results of an experiment where rotational and linear misregistrations were combined. A series of random linear shifts and rotations were applied together, with combinations of P-Zernikes following f^{-2} spectra as the incoming phase. We present results for the number of P-Zernike modes limited to 40 and limited to 50 modes (as shown in the legend). Similarly to section 3.1, we compared the $RMSE_{ratio}$ resulting from all misregistrations applied in combination to the quadratic sum of the $RMSE_{ratio}$ from the misregistrations applied separately ($RMSE_{quadSum}$, see equation (3)).

$$RMSE_{quadSum} = \sqrt{RMSE_{ratio_x}^2 + RMSE_{ratio_y}^2 + RMSE_{ratio_\theta}^2} \quad (3)$$

where $RMSE_{ratio_\theta}$ is the $RMSE_{ratio}$ when the rotation is applied with no linear shift. It can be seen in the figure that, for all rotation angles and for linear shifts limited to 0.1 actuator pitch (0.252 mm), they are approximately equal i.e., $RMSE_{quadSum} = RMSE_{ratio}$. Limited the correction to the first 40 Zernike modes (as opposed to 50) greatly reduces the residual error by approximately half.

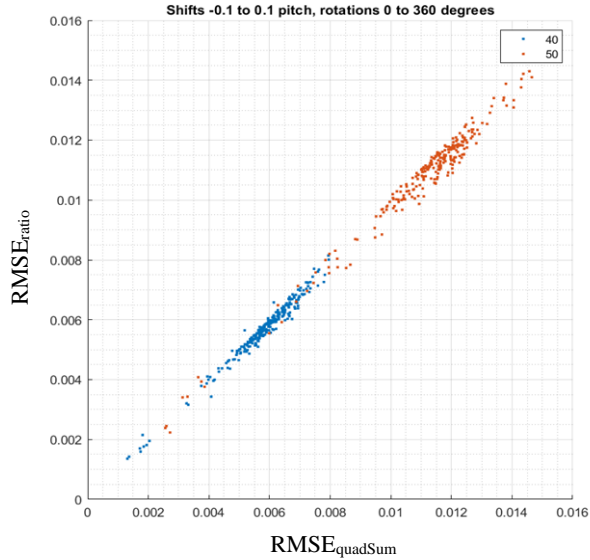


Figure 3-6: $RMSE_{ratio}$ of modes added in quadrature ($RMSE_{quadSum}$) against $RMSE_{ratio}$ of combined misregistrations. Random shifts within 0.1 actuator pitch (0.252 mm) and random rotations between 0 and 360°. NCPA following f^{-2} spectrum.

HARMONI will suffer from unwanted linear misregistrations between LODM and CalDM. In addition, the 2 DMs will be rotated with respect to one another depending on the IFS (i.e., the science path) rotation. Finally, we investigated the effect of applying increasingly large linear misregistrations at a series of rotational misregistration angles between 0° and 90°, with combinations of NCPA following an f^{-2} spectra. The P-Zernike were limited to 50 modes, as per HARMONI's requirements. Figure 3-7 shows the mean and standard deviation for $RMSE_{ratio}$ as a function of rotation angle for 4 different linear misregistration distance ranges. The linear misregistrations follow a uniform distribution within the range specified. We see that, in all cases, the $RMSE_{ratio}$ is approximately constant when the rotation angle is in the range 10° to 80°. Even in the worst case (shift from 0.4 to 0.5 actuator pitch), the average error is $\leq 2\%$ of incoming WFE and $\leq 3\%$ within 3σ (or 99.7% of the cases).

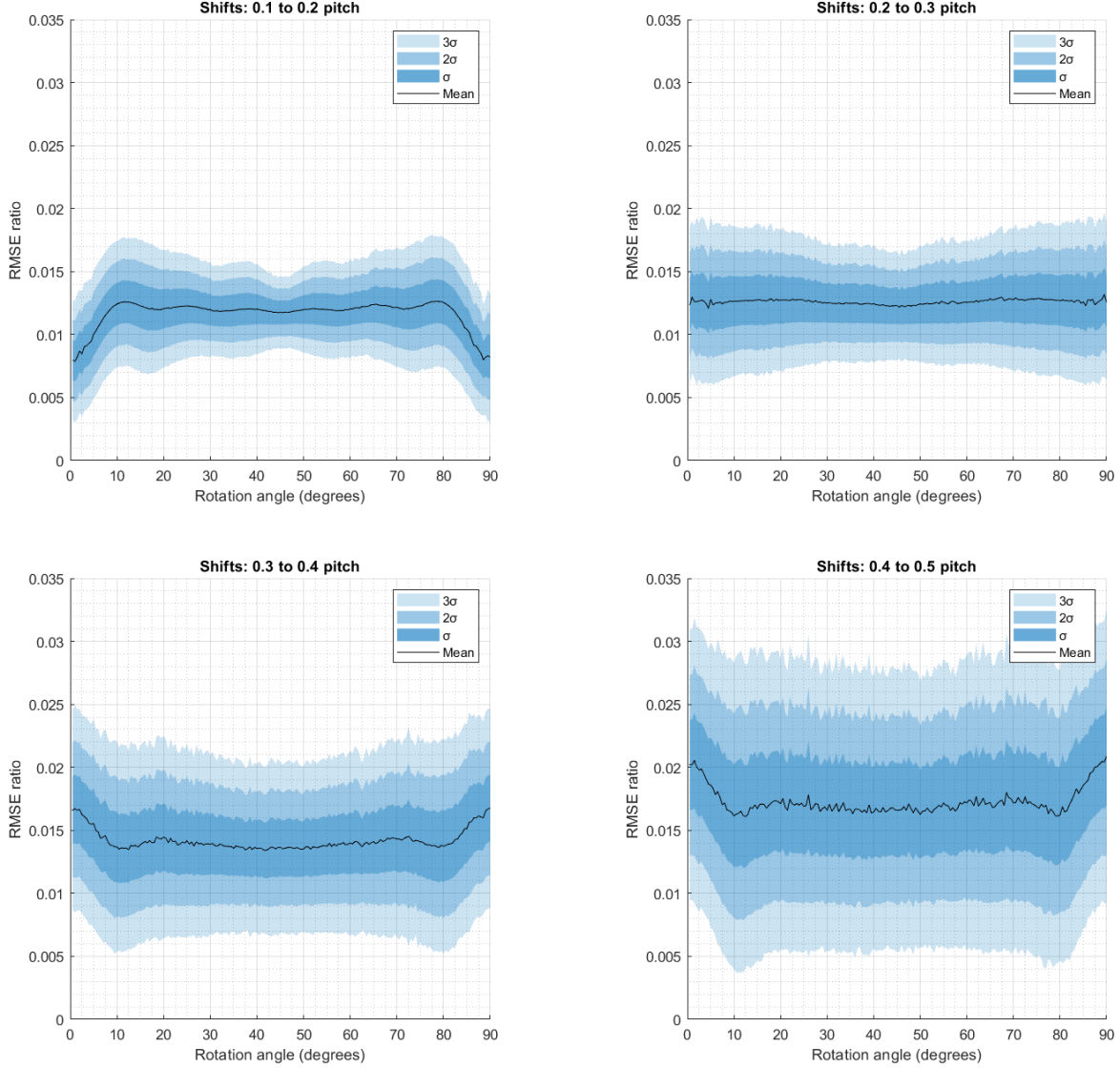


Figure 3-7: Rotation angle against $RMSE_{ratio}$ for random linear shifts in the range 0.1 to 0.2 actuator pitch (top left), 0.2 to 0.3 (top right), 0.3 to 0.4 (bottom left) and 0.4 to 0.5 (bottom right). P-Zernike modes cropped at 50, random f^{-2} spectrum incoming phases.

4. CONCLUSIONS AND NEXT STEPS

In this paper, we discussed the impact of DM misregistrations between HARMONI’s calibration DM used to probe NCPA, and the LODM used for NCPA correction. The same ALPAO DM97-25 was selected for both DMs. Three misregistrations we studied between CalDM and LODM: shifts, rotation, and magnification. To simulate realistic NCPAs, we used a series of Zernike modes projected on the DM with an f^{-2} spectrum. These modes were limited to the first 50, as HARMONI will not correct modes of higher order than this.

We found that Zernike modes with high spatial frequencies around their edges have the worst fitting errors and are highly sensitive to DM misregistration. When DM rotations between 10° and 80° are combined with random shifts within 0.5

actuator pitch (1.25 mm), the maximum error is $\leq 2\%$ of NCPAz on average and $\leq 3\%$ within 3σ . This is deemed to be sufficient for high-quality NCPA estimation and correction for HARMONI.

Our next steps are to investigate modes that may have better behaviour along the edge of the aperture (e.g., Karhunen-Loève or disk-harmonic modes) to reduce the impact of the badly fitted modes that have the worst impact on misregistrations.

ACKNOWLEDGEMENTS

HARMONI is an instrument designed and built by a consortium of British, French, and Spanish institutes in collaboration with ESO.

REFERENCES

- [1] Thatte, N. A., et al., "HARMONI at ELT: Overview of the capabilities and expected performance of the ELT's first light, adaptive optics assisted integral field spectrograph". In Ground-based and Airborne Instrumentation for Astronomy IX, Volume 12184 (2022) <https://doi.org/10.1117/12.2628834>
- [2] Schwartz N., et al., "HARMONI at ELT: adaptive optics calibration unit from design to prototyping," Proc. SPIE 12185, Adaptive Optics Systems VIII, 121855E (29 August 2022); <https://doi.org/10.1117/12.2627247>
- [3] Conan, R. and Correia C., "Object-oriented Matlab adaptive optics toolbox." Adaptive optics systems IV. Vol. 9148. SPIE, 2014. <https://doi.org/10.1117/12.2054470>